Surface-wave propagation across the Mexican Volcanic Belt and the origin of the long-period seismic-wave amplification in the Valley of Mexico

N. M. Shapiro,[1] M. Campillo,[1] A. Paul,[1] S. K. Singh,[2] D. Jongmans[3] and F. J. Sánchez-Sesma[4]

[1] *Laboratoire de Géophysique Interne et Tectonophysique, UA CNRS 733, Université Joseph Fourier, Grenoble, France*

[2] *Instituto de Geofísica, Universidad National Autónoma de México, México DF, Mexico*

[3] *Laboratoire de Géologie de l'Ingénieur et d'Hydrogéologie, Université de Liège, Liège, Belgium*

[4] *Instituto de Ingenería, Universidad National Autónoma de México, México DF, Mexico*

SUMMARY

A network of nine broad-band seismographs was operated from March to May 1994 to study the propagation of seismic waves across the Mexican Volcanic Belt (MVB) in the region of the Valley of Mexico. Analysis of the data from the network reveals an amplification of seismic waves in a wide period band at the stations situated in the southern part of the MVB.

The group velocities of the fundamental mode of the Rayleigh wave in the period range 2–13 s are found to be lower in the southern part of the MVB than in its northern part and in the region south of the MVB. The inversion of dispersion curves shows that the difference in group velocities is due to the presence of a superficial low-velocity layer (with an average S-wave velocity of 1.7 km s^{-1} and an average thickness of 2 km) beneath the southern part of the MVB. This low-velocity zone is associated with the region of active volcanism.

Numerical simulations show that this superficial low-velocity layer causes a regional amplification of 8–10 s period signals, which is of the same order as the amplification measured from the data. This layer also increases the signal duration significantly because of the dispersion of the surface waves. These results confirm the hypothesis of Singh *et al.* (1995), who suggested that the regional amplification observed in the Valley of Mexico is due to the anomalously low shear-wave velocity of the shallow volcanic rocks in the southern MVB

Key words: broad band, numerical techniques, Rayleigh waves, seismic-wave propagation, Valley of Mexico, volcanic activity.

INTRODUCTION

The strong amplification of seismic waves in the Valley of Mexico has been investigated by numerous authors (a summary of studies on this topic can be found in Singh *et al.* 1995). A large part of this amplification is due to the shallow crustal structure, especially the presence of recent, very soft lake sediments beneath part of the valley. The models, which only take into account shallow, soft sediments, give a relatively good agreement between observed and simulated amplifications but fail to explain the long duration of ground motion. Several hypotheses have been proposed to explain the unusual duration. Singh & Ordaz (1993) proposed that the origin of the long coda in the region of the Valley of Mexico is not in

the shallow structure but in the structure at regional scale. The existence of such a structure was inferred from the observation of a regional amplification (Ordaz & Singh 1992; Singh *et al.* 1995). Singh *et al.* (1995) suggested that the smaller-than-normal shear-wave velocities in volcanic rocks could be the cause of this regional amplification.

The Mexican Volcanic Belt (MVB) is a prominent structural element in the geology of Mexico (Fig. 1). The geochronological data (Demant 1981; Robin 1981) show that the volcanic rocks forming the MVB are Pliocene and Quaternary in age. With its E–W orientation, the MVB intersects other geological structures of Mexico. The MVB is surrounded by Mesozoic rocks of the Sierra Madre Oriental in the north, and the Sierra Madre del Sur in the south. It is generally accepted that the
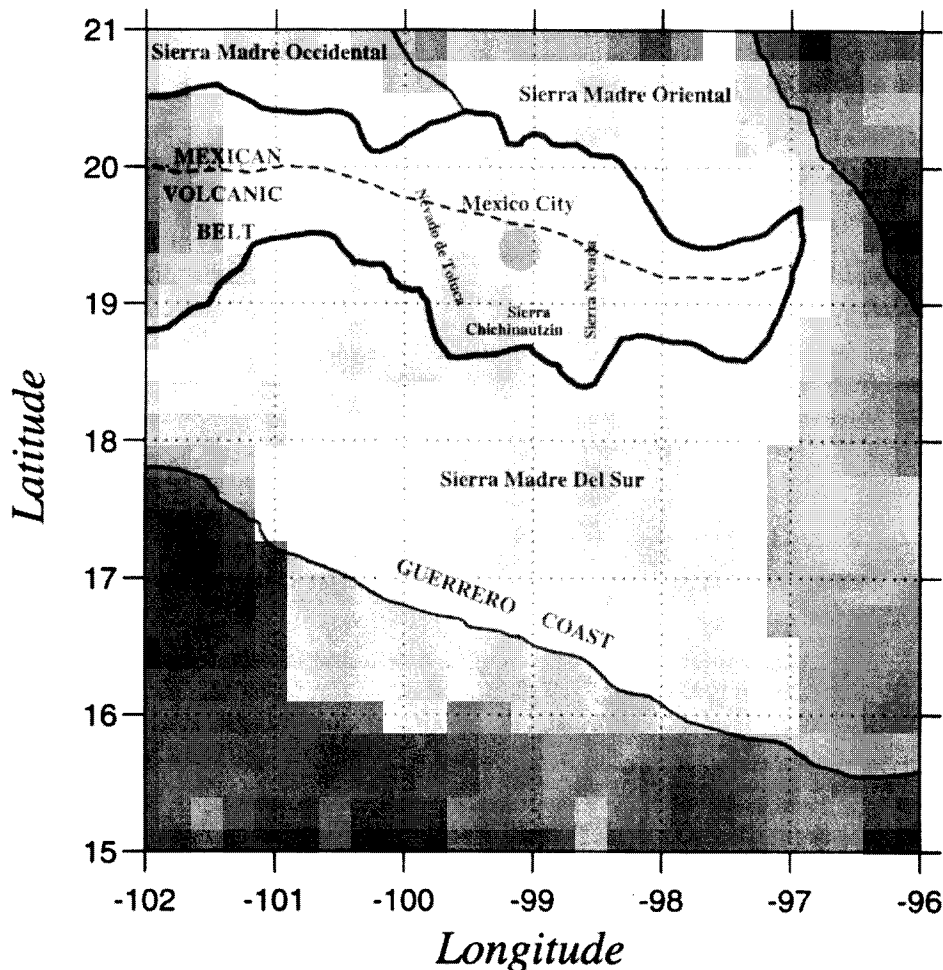
Figure 1. Structural map of southern Mexico (modified from Tardy 1980). The solid line shows the boundaries of the Mexican Volcanic Belt (MVB). The dashed line shows the limit between the zone of actual volcanism and the northern non-active part of the MVB (Robin 1981).

andesitic volcanism of the MVB is due to the subduction of the Cocos plate under the North American continent. The zone of present-day volcanic activity is located in the southern part of the MVB. In the region of the Valley of Mexico, the MVB is composed of three main elements: Nevado de Toluca to the west, Sierra Chichinautzin to the south and Sierra Nevada to the east. The northern part of the MVB consists of rocks more than 2.5 Myr old and is presently not active. The migration of the volcanism from the north to the south is associated with the acceleration of the Cocos plate subduction between 4 and 5 Myr BP (Robin 1981).

To verify experimentally if the regional amplification in the Valley of Mexico is caused by the regional structure, a 300 km long profile of nine broad-band, three-component seismographs was installed across the MVB in an approximately N–S direction. The experiment lasted 3 months (March to May 1994). Its goal was to study seismic waves originating from earthquakes occurring along the Guerrero subduction zone and propagating through the MVB, including the Valley of Mexico.

The location of the broad-band stations is shown in Fig. 2 and given in Table 1. Two of these (UNAM and Iguala) are permanent stations. The others are portable Reftek recorders connected to Guralp CMG40 sensors which were installed for the duration of the experiment.

Table 1. Station locations. UNAM and Iguala are permanent, very broad-band stations operated by UNAM. Others were broad-band portable seismographs (Reftek + CMG40T seismometers) installed during the 3 months of the experiment.

Name	Begin	End	Latitude	Longitude
Iguala	permanent	permanent	18.389	−99.51
Jiutepec	24.04.1994	14.05.1994	18.975	−99.175
Tepoztlán	26.03.1994	14.05.1994	18.986	−99.075
Parres	26.03.1994	23.04.1994	19.139	−99.174
Popocatépetl	28.03.1994	15.05.1994	19.067	−98.63
UNAM	permanent	permanent	19.329	−99.178
Texcoco (lake)	30.03.1994	13.05.1994	19.465	−99.00
Texcoco (rock)	07.04.1994	13.05.1994	19.501	−98.806
Teotihuacán	27.03.1994	13.05.1994	19.69	−98.86
Actopan	27.03.1994	13.05.1994	20.33	−99.066

The network crossed the MVB perpendicular to its E–W strike. The station Actopan was located approximately at the northern limit of the MVB, while the sites Jiutepec and Tepoztlán were situated near its southern limit.

More than 30 seismic events with good signal-to-noise ratio were recorded during the experiment. In this work, we investigate the change in crustal structure across the MVB by inversion of dispersion curves of surface waves between different stations. This requires events located in a direction close
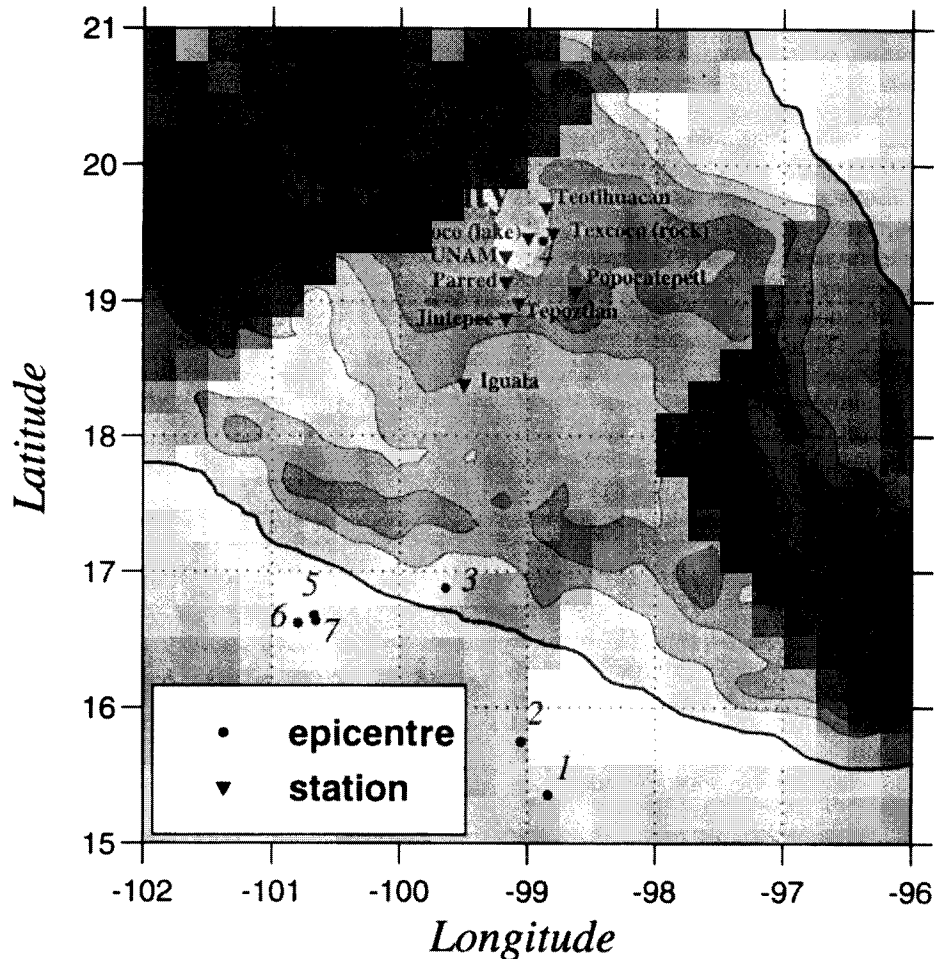
Figure 2. Topographic map of southern Mexico showing the locations of seismic stations and earthquakes used in this study. The italic numbers assigned to the events are keyed in Table 2. Note that, except for event 4, which occurred in the Valley of Mexico, all others were located near the coast of Guerrero.

to the mean azimuth of the profile (N–S) and at a distance sufficiently large for the development of relatively long-period surface waves. Such events occurred in the subduction zone near the Guerrero coast. We present the analysis of six of these events (see Table 2, events 1–3 and 5–7). Of particular interest was another small earthquake that occurred beneath Texcoco, in the suburbs of Mexico City (event 4). The locations of all events used in this study are shown in Fig. 2.

We first analysed the available seismograms in order to define the limits of the region where the amplification was observed. We then measured group and phase velocities of the Rayleigh wave in the northern and southern parts of the MVB, using the Guerrero events for periods between 5 and 13 s (henceforth called the 'long-period' range) and the Texcoco

event in the period range 2–5 s (henceforth called the 'short-period' range). The results of the measurements were used to build up composite dispersion curves for the northern and southern parts of the MVB, which were then inverted for local S-wave velocity structures. The results of the inversions were used to construct a simple model and to compute synthetic seismograms in order to verify whether the observed structure can explain the amplification—this is detailed in the final section.

ANALYSIS OF SEISMOGRAMS

We first considered the records of six events that occurred south of the MVB, near the coastline of the State of Guerrero

Table 2. Event locations.

N°	Latitude	Longitude	Year	Month	Day	Hour	Min	Sec	M
1	15.36	−99.84	1994	3	31	21	58	54	4.6
2	15.75	−99.05	1994	4	2	11	47	43	4.8
3	16.88	−99.64	1994	4	15	4	48	18	4.3
4	19.44	−98.88	1994	4	30	8	10	30	4.0
5	16.68	−100.67	1994	5	4	19	57	42	4.4
6	16.62	−100.79	1994	5	5	12	18	45	4.4
7	16.64	−100.65	1994	5	5	12	39	24	4.5

(events 1, 2, 3, 5, 6 and 7). We separated these events into three groups. The first group contains events 1 and 2, which occurred to the south of the Valley of Mexico; the second group consists only of event 3, which is located slightly to the west of the first group; and the third group contains events 5, 6 and 7, which occurred to the west of the second group (Fig. 2). The reason for such a separation is that waves emitted by events of each group and recorded by stations in our network cross slightly different regions of the Valley of Mexico.

An important observation for all the Guerrero events is the confirmation of the amplification at the sites in the volcanic belt around the period of 3 s. This is illustrated in Fig. 3, which shows bandpass-filtered (between 0.2 and 1 Hz) seismograms for event 1. The signal amplitude is larger at stations Parres, UNAM and Texcoco (lake) than at stations Iguala and Tepoztlán, which are located closer to the epicentre. The amplitude reaches its highest value at station Texcoco (lake) and then decreases at stations Teotihuacán and Actopan, located in the northern part of the MVB. This is especially clear on the horizontal components.

A careful analysis of the records shows that the signals remain amplified even at relatively long periods of 8–10 s. For event 1, this amplification can be seen in Fig. 4, especially on the horizontal components. Another interesting fact is that, for events of the first group, the amplitudes have already decreased at Teotihuacán, which is still located on volcanic rocks (see, for example, vertical and radial components for event 1 in Fig. 4).

Fig. 5 presents low-pass-filtered seismograms for event 5. For events of the third group, the amplification at long periods is observed on the horizontal components, but the amplitudes of vertical components remain almost constant at all the stations. For this event, the signal on the transverse component almost disappears in the northern part of the MVB (Actopan).

The main point deduced from seismograms of the Guerrero events is the amplification in the period range 1–10 s in the southern part of the MVB. The southern limit of the region where this amplification is observed is located near Tepoztlán and corresponds to the geographical and geological limits of the MVB. The characteristics of the signal in the northern part of the MVB change for events of the different groups. However, no strong amplification is observed at Teotihuacán and Actopan. This suggests that the northern limit of the region with amplification is situated near Teotihuacán.

Another indication of a change in the crustal structure near Teotihuacán comes from records of the small event which occurred on 1994 April 30 near Texcoco (event 4). The main feature of the seismograms of this earthquake is a great difference in the duration of the signals at different stations. The vertical-component seismograms are shown in Fig. 6 (the signal duration is the same for all three components), where the seismograms are normalized and low-pass filtered at 1 Hz. The traces recorded south of the epicentre (Iguala, Jiutepec, Tepoztlán, Popocatépetl, UNAM) are much longer than those recorded in the north (Actopan, Teotihuacán, Texcoco rock). This point is well illustrated by comparing the records at Teotihuacán and UNAM, two stations located at approximately the same distance from the epicentre (Fig. 6). The durations of the records at Tepoztlán and Jiutepec are longer than at Actopan, while the epicentral distances are about half the size. The record at Popocatépetl is shorter than at other stations in the south, but the group velocity of the most
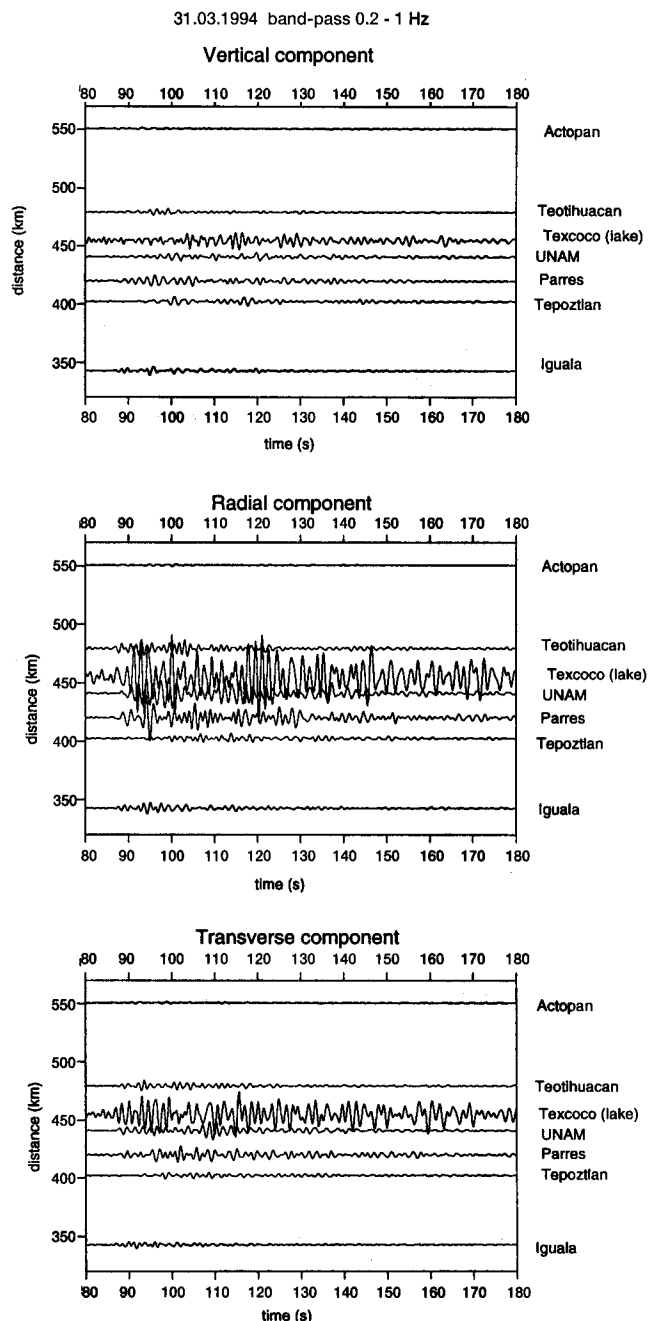

Figure 3. Seismograms of event 1 bandpass-filtered between 0.2 and 1 Hz. The abscissa is the traveltime reduced at 3.5 km s^{-1}.

energetic arrival at this station remains smaller than those at Teotihuacán and Actopan. The long duration of the record at UNAM can be explained by the fact that the travel path lies inside the Valley of Mexico, which is known to be covered by very soft lacustrine deposits. Simultaneously with this broad-band experiment, we also operated a dense array of seismometers in the vicinity of UNAM. The array analysis of this event shows that the later arrivals (after 60 s) observed at UNAM are probably refracted from the edge of the Valley of Mexico (Barker *et al.* 1996). This explanation, however, is not valid for other stations, especially the one at Popocatépetl. In
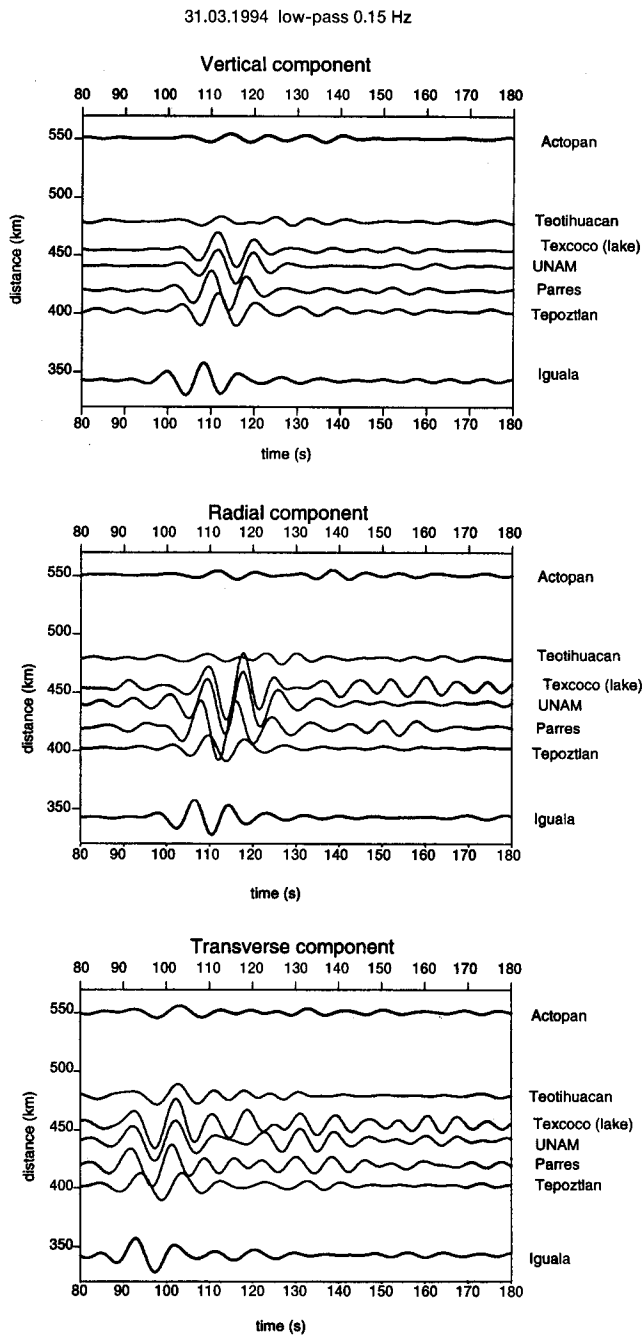
Figure 4. As Fig. 3, but low-pass-filtered at 0.15 Hz.

Figure 5. As Fig. 4, but for event 5.

this case, the travel path lies entirely outside the Valley of Mexico. This suggests the possibility of the existence of a low-velocity structure beneath the MVB.

These preliminary observations revealed an amplification in the southern part of the MVB. The southern limit of the region of observed amplification is situated near Tepoztlán, and the northern limit is situated near Teotihuacán. The existence of the northern limit is also indicated by the change in the duration of the records of the Texcoco event. Both amplification and long signal duration can be explained by the existence of a layer of low-velocity material in the southern part of the MVB. In order to verify this hypothesis, we
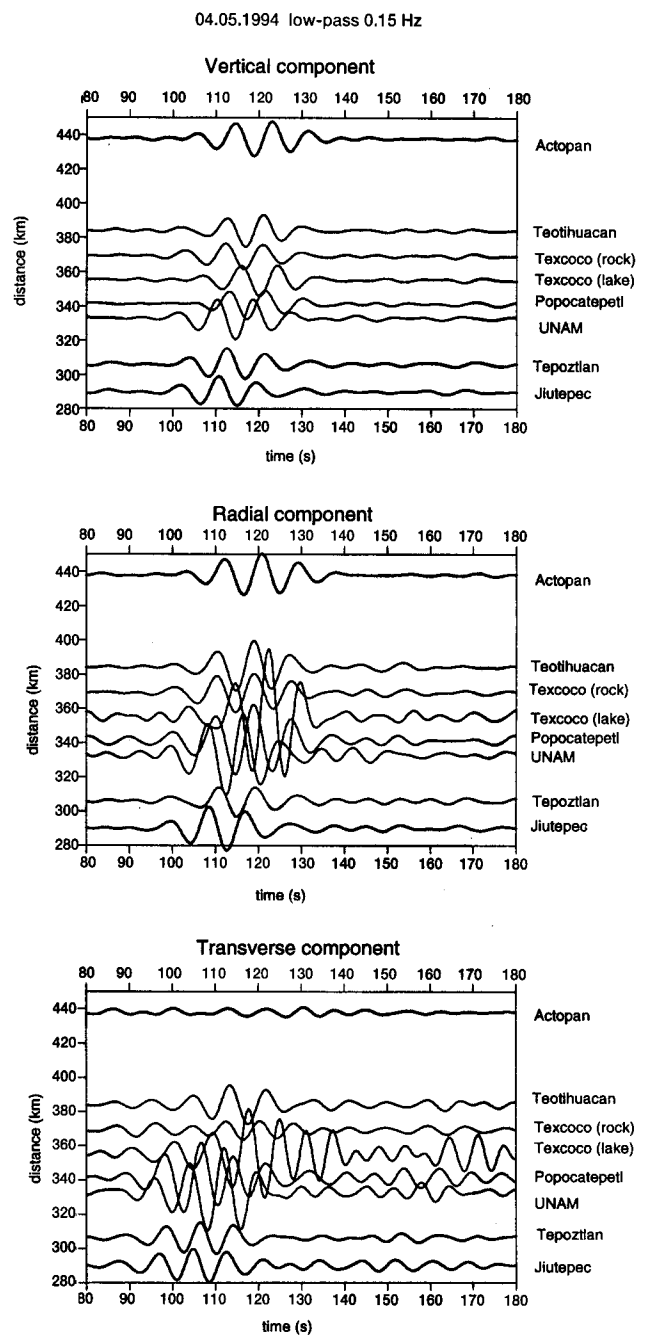
measured group and phase velocity dispersion curves of the Rayleigh wave inside and outside the amplifying zone in the southern part of the MVB. The limits of this zone (Fig. 7) were tentatively assigned from the analysis of seismograms described above.

RAYLEIGH-WAVE IDENTIFICATION

Before measuring the group and phase velocity dispersion of the Rayleigh wave, we selected in each record the time interval and the period range in which this type of wave is dominant and, if possible, extracted this wave from the signal. A fre-
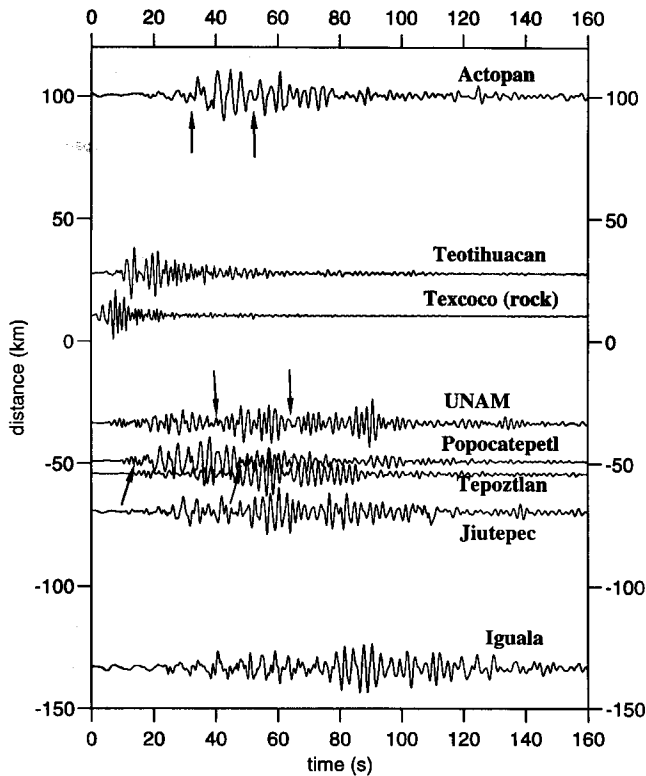
Figure 6. Vertical-component seismograms of the Texcoco event (event 4). The seismograms are low-pass-filtered at 1 Hz. The sign of the distance depends on the station location with respect to the epicentre: positive to the north, and negative to the south. Note the longer signal duration to the south. Arrows show arrivals of the Rayleigh wave at Actopan, UNAM and Teotihuacán, which are used for the measurement of group velocity.

Figure 7. Map showing amplifying zone beneath the southern MVB. The southern and northern limits of the zone are situated near Tepoztlán and Teotihuacán, respectively. The existence of the northern limit is supported by a change in the duration record of the Texcoco event (see text).
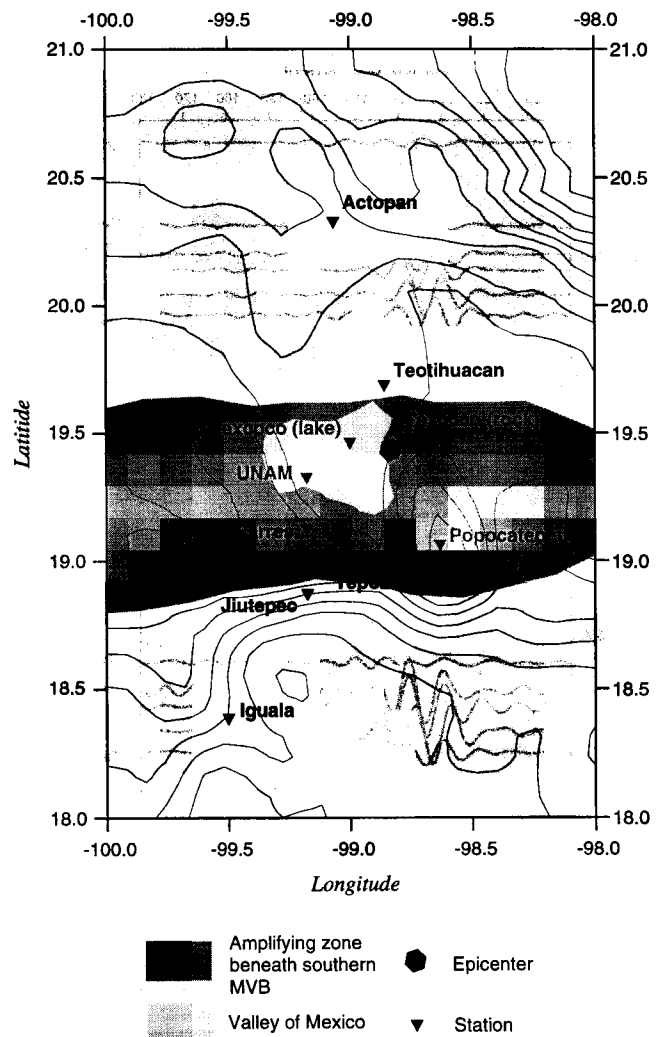
quency–time analysis (e.g. Levshin *et al.* 1989; Dziewonski, Bloch & Landisman 1969) is used to characterize the dispersed signals (see Appendix A).

The period–time diagrams for vertical component records of the Texcoco event at stations Popocatépetl and Actopan are shown in Figs. 8(a) and (b), respectively. They show that the signal consists of a set of different arrivals. The most energetic arrival shows slight dispersion. The polarization analysis (Levshin *et al.* 1989) shows that this first arrival can be identified as a Rayleigh wave. This type of analysis was performed on all the records. In Fig. 6, the parts of the seismograms identified as Rayleigh waves at stations Popocatépetl, Actopan and UNAM are indicated with arrows. These records were used later for velocity measurements.

The same type of analysis was applied to the records of the Guerrero events. One example (vertical component record of event 7 at Teotihuacán) is presented in Fig. 8(c). Polarization analysis shows that the most energetic arrival is a Rayleigh wave. It does not show important dispersion between 5 and 20 s.

A significant enhancement of the individual period–time diagrams can be obtained by logarithmic stacking (Campillo *et al.* 1996), which is described in Appendix A.

We selected events 5, 6 and 7 to perform this stacking because of their close epicentral locations, confirmed by the similarity of the three seismograms at each of the stations. This similarity allowed us to correct for possible errors in the

origin times. For the stacking in the period–time domain, we need the same absolute timescale for different events. To satisfy this requirement, we selected one of the events as a reference (event 7) and corrected the origin time of all the others with respect to this reference. We measured the time delay between two records using a linear regression on the phase of the cross-spectrum (Poupinet *et al.* 1984). We then calculated the correction for the origin time of each event as the average value, for all stations, of the time delays between records of this event and the reference event. We checked that this delay was the same at the different stations within about 0.2 s. The hypothesis of the close location of the different events was verified by the good linearity of the phase of the cross-spectra (in the case of a significant difference in travel paths, this phase is affected by the dispersion).

After applying the time corrections, we constructed stacked period–time diagrams for each station and measured the mean dispersion of the group time. At each station, a stacked diagram was calculated using the diagrams of vertical and radial components for each of the three events. The measurements
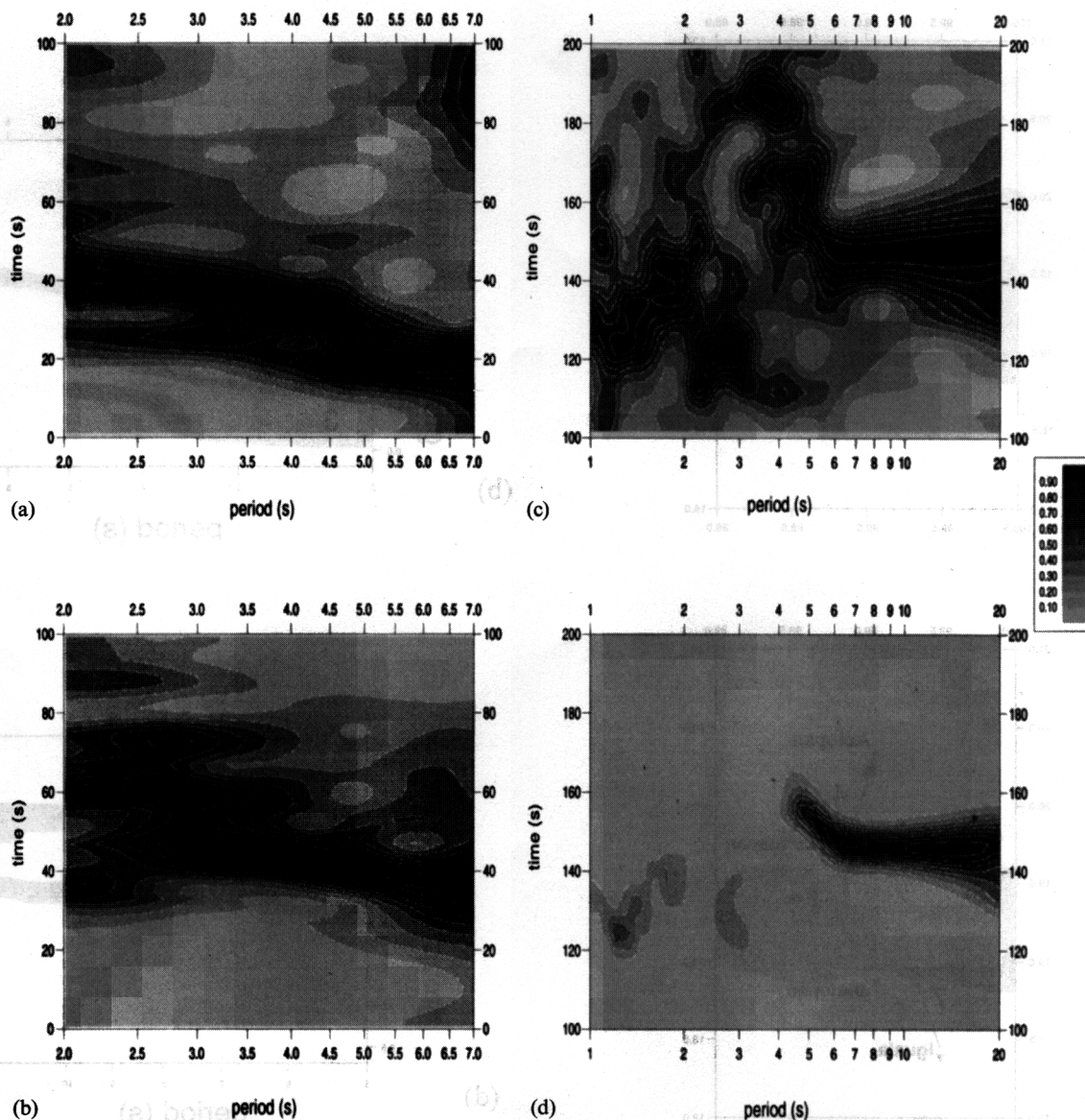
Figure 8. Some examples of period–time diagrams used for the identification of the Rayleigh wave and for the group velocity measurement. (a) Period–time diagram for the vertical-component record of the Texcoco event at Popocatépetl. Polarization analysis shows that the first ridge corresponds to the Rayleigh wave. The corresponding arrival on the seismogram is shown by arrows in Fig. 6. (b) As (a), but recorded at Actopan. (c) Period–time diagram for the vertical-component record of event 7 at Teotihuacán. (d) Stacked diagram at Teotihuacán (records of the vertical and radial components of events 5, 6 and 7). The period–time domain corresponding to the fundamental mode of the Rayleigh wave is well defined between 5 and 20s.

were performed at seven stations: Jiutepec, Tepoztlán, UNAM, Texcoco (lake and rock sites), Teotihuacán and Actopan. Station Iguala was not working during this period and station Popocatépetl could not be used because the GPS receiver was unlocked. Fig. 8(d) shows the stacked period–time diagram at Teotihuacán. Note that the period–time domain of the Rayleigh wave is better defined in the stacked diagram than in the diagram of an individual record (Fig. 8c).

The results of logarithmic stacking are as follows. For all stations the amplitudes of stacked diagrams are high for periods between 5 and 13 s. For the stations Jiutepec and Tepoztlán, the amplitudes of the resulting diagrams remain high for periods as low as 2.5 s. Conversely, the amplitudes are low at periods less than 5 s at stations located inside the MVB and to the north of it. These low amplitudes may be due to the presence of strong heterogeneities at kilometric scale beneath the volcanic belt.

Summarizing the results of frequency–time analysis, a Rayleigh wave can be distinguished with sufficiently high amplitudes on all seismograms. For the Guerrero events, this wave is observed at periods of 5–13 s. For the Texcoco event, it is observed at periods of 2–5 s, except at Actopan where it is seen up to periods of 7 s because of a larger epicentral distance (100 km).

VELOCITY MEASUREMENTS

Group velocities at short periods (2–5 s)

The records of the Texcoco event were selected to measure group velocities in three different zones (Fig. 9a). Because of
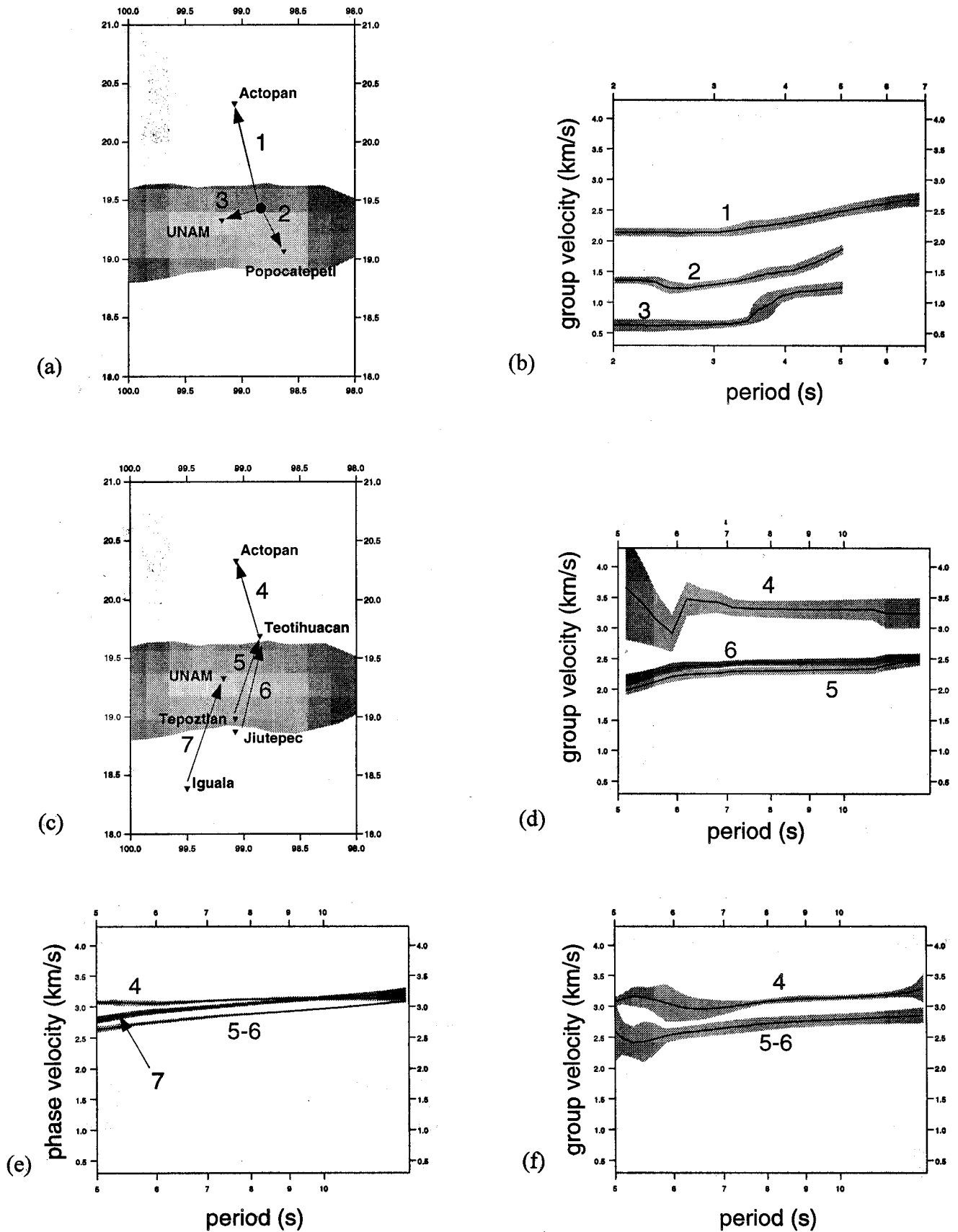
Figure 9. Results of the velocity measurements. (a) Paths used for the measurements of group velocities at short periods. (b) Group velocities at short periods. (c) Paths used for the velocity measurements at long periods. (d) Group velocities at long periods. (e) Phase velocities at long periods. (f) Group velocities at long periods deduced from the phase velocities shown in (e).

Love-wave contamination and enhanced mode coupling on the horizontal components (Stange & Friederich 1992), we used only the vertical components for the measurement of velocities of the Rayleigh wave at short periods. The records at Actopan, Popocatépetl and UNAM were used to characterize the northern part of the MVB, the zone of active volcanism, and the Valley of Mexico, respectively (paths 1, 2 and 3 in Fig. 9a). We did not use the other records for the group velocity measurement because travel paths cross different regions and measurement results would have been difficult to interpret.

The procedure used in measuring the group velocity is outlined in Appendix B. The results of the analysis are shown in Fig. 9(b). The solid lines show the group velocities obtained with eq. (B1) and the shaded areas show the errors estimated from one-record period–time diagrams. The results of the measurement confirm the previous suggestion that the velocities south of the MVB are lower than those in the north. At periods of 2–3 s, the group velocity is about 2.2 km s^{-1} in the northern part of the MVB, and about 1.4 km s^{-1} in the southern part.

Group velocities at long periods (5–13 s)

We used records of the Guerrero events and eq. (B2) to determine group velocities in the northern and southern parts of the MVB. Group times at each station were defined using stacked period–time diagrams. The diagrams for individual records were not sufficiently narrow to allow a precise estimation of the group time.

We measured group velocities between Teotihuacán and Actopan to characterize the northern part of the MVB (path 4 in Fig. 9c). Jiutepec, Tepoztlán and Teotihuacán were used to obtain mean velocities inside the volcanic belt (paths 5 and 6 in Fig. 9c). Other possible combinations of stations were not used because they correspond to very small interstation distances or to paths crossing different zones. The results of the group velocity measurements are shown in Fig. 9(d). As in Fig. 9(b), solid lines show average dispersion curves obtained with eq. (B2) and shaded areas show the standard deviation deduced from eq. (A4). In spite of the large uncertainties, the difference in group velocities between the southern and northern parts of MVB at long periods is well resolved. We find once again that group velocities are larger in the northern part of the MVB. Unfortunately, we cannot perform similar measurements for the zone situated south of the MVB because of the lack of data at Iguala.

Phase velocities at long periods

We also performed measurements of interstation phase velocities for the same pairs of stations, applying the cross-spectrum method which is outlined in Appendix C (eq. C2) with preliminary filtering in the frequency–time domain.

The results of measurements for the paths 4, 5, 6 and 7 in Fig. 9(c) are presented in Fig. 9(e). The error in the measurement is represented by the shaded area, which has a width equal to one standard deviation. In agreement with the previous results, the velocities south of the MVB are found to be lower than those in the north.

We measured phase velocities between Iguala and UNAM (path 7 in Fig. 9c) using records of vertical and radial compo-

nents of events 1, 2 and 3. Unfortunately, the measurement between Iguala and Jiutepec or Tepoztlán could not be performed accurately because of the difference in the instrument response of the very broad-band seismographs at Iguala and the portable seismograph. The path Iguala–UNAM does not only characterize the southern zone but it also partly crosses the MVB. The velocities obtained for this path (Fig. 9e, curve 7) are intermediate between those in the northern and southern parts of the MVB. This result allows us to assume that the regions south and north of the MVB have similar upper crustal structures.

For the southern part of the MVB, the group velocities measured directly (Fig. 9d) have smaller values than those deduced from the phase velocities through eq. (C3). The opposite is true to the north of the MVB. The main observation, however, that the group velocities beneath the southern part of the MVB are lower than in its northern part is verified.
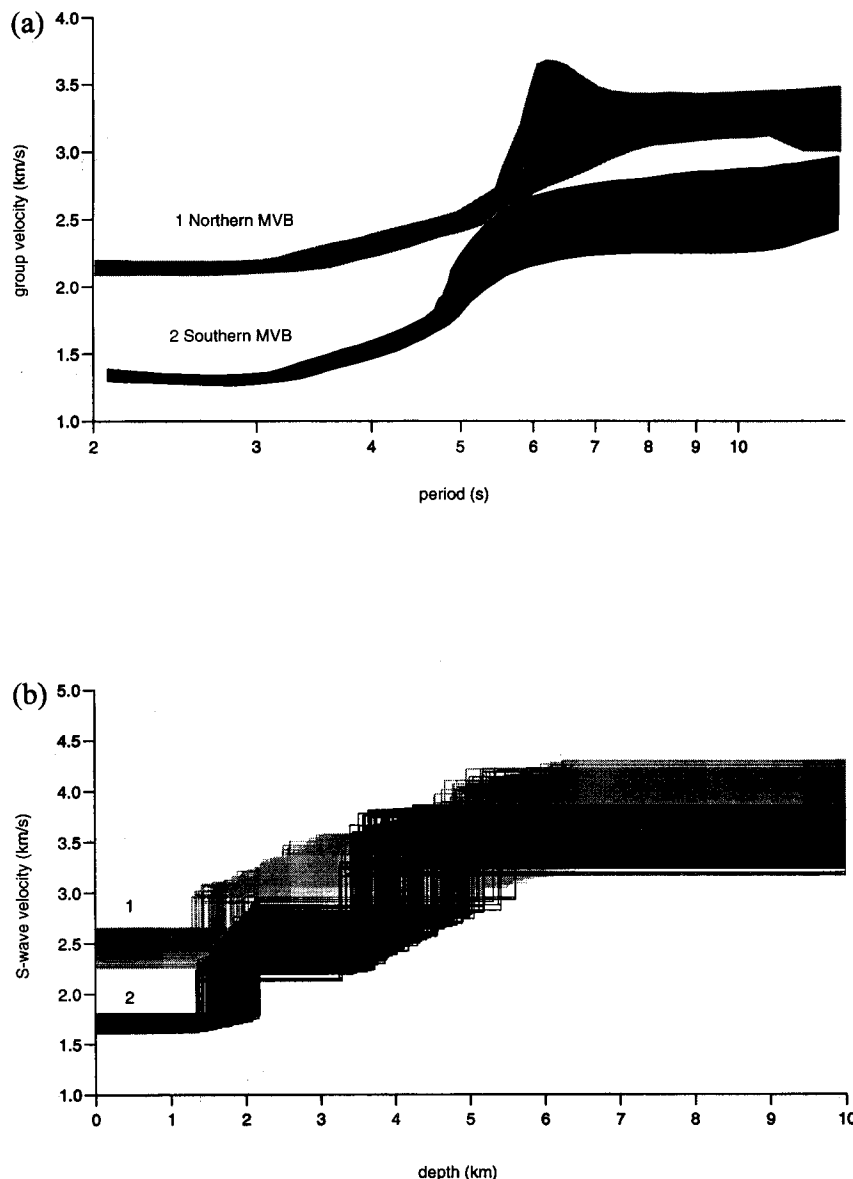
INVERSION OF GROUP VELOCITY DISPERSION FOR THE CRUSTAL STRUCTURE

The different measurements of the group velocity dispersion indicate the existence of a low-velocity zone beneath the southern part of the MVB. The group velocities in the northern part are higher than those in the southern part in the period range between 2 and 13 s. South of the MVB, the crustal structure seems to be similar to that in the north. This similarity is supported by the similarity between the group velocities measured at periods 5–13 s for the northern part of the MVB and the mean group velocity dispersion found by Campillo *et al.* (1996) for the region between the Guerrero coast and Mexico City.

By combining the measurements at short periods (from the Texcoco event) and long periods (from the Guerrero events), we constructed a composite dispersion curve. The dispersion curve inside the low-velocity zone was obtained by combining the curve for the path Texcoco–Popocatépetl (at short periods) with the curve for the paths Jiutepec–Teotihuacán and Tepoztlán–Teotihuacán (at long periods). The dispersion curve for the northern part of the MVB is a combination of the measurements for the paths Texcoco–Actopan and Teotihuacán–Actopan.

The resulting dispersion curves for the northern and southern parts of the MVB are shown in Fig. 10(a). We do not obtain a single curve for each region but an area of confidence using the uncertainties of measurements. At periods of 5–13 s, we have two types of measurement of the group velocity, one obtained from logarithmic stacking, and the other deduced from phase velocities. Both measurements are taken into account for the composite dispersion curve. As a consequence, the uncertainty of the measurement of group velocities at these periods is large.

We inverted these resulting dispersion curves for the velocity structure in two steps. First, we performed a gradient inversion (Herrmann 1987) of the average dispersion curve. The initial model was based on the velocity model found by Campillo *et al.* (1996). It includes five layers with constant velocities. The initial depths of the interfaces were 2, 5, 17 and 45 km. We performed the inversion for the S-wave velocity in each layer and for the depth of the interfaces. The density and Poisson ratio were kept fixed in each layer. In the second step,

Figure 10. (a) Combined group velocity dispersion curves for the two regions: 1, northern part of the MVB; 2, southern part of the MVB. (b) Velocity models considered as acceptable for these two zones.

we estimated the uncertainty of the results obtained by linearized inversion. Starting from the model obtained by gradient inversion, we generated a set of new ones by randomly changing the S-wave velocity of each layer in the range [−0.5 km s⁻¹, +0.5 km s⁻¹], and randomly changing the depth of the interfaces in the range [−0.3 km, +0.3 km]. For each new model, we calculated group velocities of the fundamental mode of the Rayleigh wave using Herrmann's (1987) subroutines. When these group velocities were found inside the area of confidence (Fig. 10a), the corresponding model was kept and the search was continued in the vicinity of this model. The reason for using this two-step procedure is its efficiency in the exploration of a large model space. An alternative to this approach is to use a genetic algorithm (Lomax & Snieder 1994, 1995).

A first test showed that the uncertainty on the velocity in the deep layers (>10 km) is large and the deep crustal structure

is not resolved by our data. To study the uncertainties on the shallow structure, we generated a set of models where the S-wave velocity and the interface depths change only in the three shallow layers.

More than 10 000 models were tested and more than 500 of them were found to be acceptable for each of the two regions (the southern and the northern parts of the MVB). All acceptable models are plotted in Fig. 10(b). Despite the large uncertainties, the difference in the shallow (<2 km) structures of the two regions is well resolved. The observed difference in group velocities between the southern and northern parts of the MVB is due to the presence of a superficial low-velocity layer with an average thickness of 2 km in the southern part. The S-wave velocity in this layer is the single parameter for which the inversion gives a relatively small uncertainty. It is about 1.7 km s⁻¹. This is in agreement with a refraction study in the Valley of Mexico by Havskov & Singh (1978), who reported

an upper layer of 2 km thickness with a *P*-wave velocity of 2.9 km s^{-1}. Jongmans *et al.* (1997) studied the *P*-wave velocity of the volcanic rocks in the region of Mexico City using seismic refraction techniques and also obtained low values. Thus, we can associate the low-velocity zone with the volcanic layer.

We conclude that a superficial low-velocity layer exists in the active part of the MVB. Our data show that its thickness is about 2 km. The N–S extension of this layer can be roughly estimated as the distance between Teotihuacán and Tepoztlán, which is about 80 km. We think that the difference in the upper crustal structure between the northern and southern parts of the MVB is due to the difference in the type and age of the volcanism (Robin 1981).

NUMERICAL SIMULATIONS

In the previous section, we have seen that the region where the amplification of seismic waves is observed is characterized by the presence of a low-velocity layer beneath the surface. We now test whether this superficial low-velocity layer is the cause of the regional amplification.

To determine the influence of this layer on the propagation of the Rayleigh wave, synthetic seismograms were calculated using the 'indirect boundary integral method' described by Pedersen, Campillo & Sánchez-Sesma (1995). We considered a model with a single layer of 2 km thickness and with an *S*-wave velocity of 1.7 km s^{-1} overlying a half-space with a velocity of 3 km s^{-1} (see Table 3 for model parameters). The width of the low-velocity structure is 80 km. The incident wave is a Rayleigh wave. The time function of the incident signal is a 5 s Ricker wavelet. The origin of the spatial coordinate is at the centre of the low-velocity layer and its edges are located at 40 km and −40 km. 21 receivers were located between the positions −80 km and 80 km.

In Figs. 11(a) and (b), we present the synthetic seismograms filtered in the same way as the records of event 1 in Figs 3 and 4, and event 5 in Fig. 5. Low-pass filtered seismograms of the observed data (Figs. 4 and 5) and of the synthetics (Fig. 11a) have similar characteristics. The shape of the signal is roughly the same at all the receivers, but the amplitudes are larger above the low-velocity layer. A discrepancy between data and synthetics is the strong attenuation of the observed signals in the northern part of the MVB for events 1 and 2.

The high-frequency synthetics (Fig. 11b) cannot be directly compared with the data. In the simulation, the incident wave-field consists of the fundamental mode of the Rayleigh wave alone, whereas the wavefield in the real data is much more complicated. An interesting feature of these high-frequency synthetics is the generation of a packet of dispersed waves at the edge of the upper layer (Volcanic Belt). The dispersion of surface waves inside the low-velocity layer induces a strong increase of the signal duration, especially on periods around 3 s where a very well-defined Airy phase of the Rayleigh wave is observed.

We do not know the precise geometry of this layer since the

inversion only gives its average thickness. It seems reasonable to assume that a volcanic chain is a strongly heterogeneous structure and not a homogeneous layer. In order to test the influence of a possible heterogeneity on the signal, we constructed a model where we defined the base of the low-velocity layer as a random irregular function with an average wave-length of 10 km and a maximum possible deviation of 1.5 km from the mean value. This 2-D irregular model is shown in Fig. 12.

At long periods (Fig. 12a), the seismograms are very similar to those presented in Fig. 11(a), with a similar amplification in the low-velocity layer. At short periods (Fig. 12b), the form of the packet of dispersed waves above the low-velocity layer is different from Fig. 11(b) and its duration is not as long as for the model with the homogeneous layer. The irregularity of the base does not allow a constructive interference inside the low-velocity layer. Consequently, we do not observe a well-defined Airy phase. However, the increase of signal duration due to the dispersion of surface waves inside the low-velocity layer is still observed. We do not have the data which would allow us to verify which of two models is the closest to the actual structure of the MVB. Nevertheless, we prefer the second one because it is difficult to imagine the volcanic chain as a perfectly homogeneous layer.

In Fig. 13, we compare long-period spectral amplification (8–10 s) of the synthetic seismograms computed for the model with the low-velocity layer with irregular base at receivers located above this layer with the amplification observed in the southern part of the MVB. For the synthetic data, the first receiver is taken as the reference. For the observed data, Iguala site is taken as the reference for events 1, 2 and 3, and Jiutepec is used as the reference for events 5, 6, and 7. A correction for the geometrical spreading is made assuming surface-wave propagation for the observed data. We only consider the amplification at long periods (8–10 s) for two reasons:

(1) At smaller periods the observed signals do not consist of the fundamental mode of the Rayleigh wave alone.
(2) Short-period synthetics cannot be compared with the observation since very shallow structures play a prominent part in the amplification of seismic waves.

The comparison in Fig. 13 is fair inside the low-velocity zone (−40 to 40 km). The horizontal component of the synthetics is amplified by a factor of about 1.7. The amplification of the vertical component depends on the topography of the base of the low-velocity layer. The amplification of the synthetic seismograms is of the same order as that of the observed ones. We do not pretend to simulate the regional amplification exactly, because of the lack of information on the detailed structure of the volcanic layer. The influence of the small-scale shallow structure must also be considered, particularly for stations UNAM and Texcoco (lake site). Another important point is that the volcanic chain is a 3-D structure. For example, the model does not explain the fact that the amplitude of the Rayleigh wave at Teotihuacán and Actopan is strongly reduced for events 1 and 2. This could be due to the local heterogeneity in the region of Texcoco. For other events along the Guerrero Coast, with more westerly locations, the travel paths do not cross this region and the amplitude reduction in the northern part of the MVB is not observed.

The main conclusion obtained from the numerical simu-

Table 3. Parameters of the model used in the numerical simulation.

Layer	Vp (km/s)	Vs (km/s)	ρ (g/cm^3)
1	2.93	1.71	2.1
2	5.20	3.00	2.4

(a) low-pass at 0.15 Hz

(b) band-pass 0.2-1 Hz
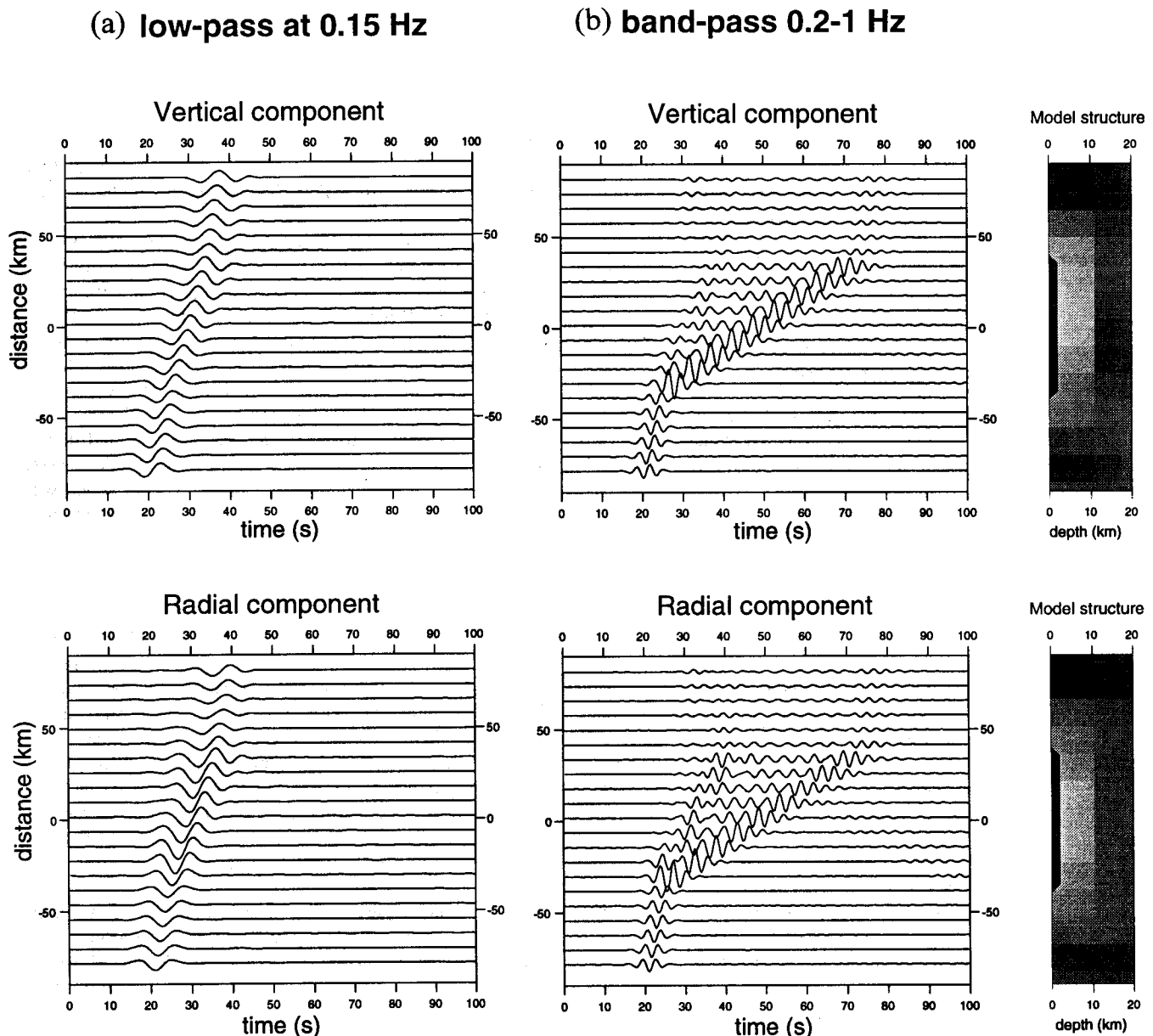
Figure 11. Synthetic seismograms computed for a shallow low-velocity layer with a flat basement. The abscissa is the time reduced to a velocity of 3.5 km s^{-1}. The model cross-section is plotted on the right-hand side of each section. The parameters of the model are shown in Table 3. (a) Seismograms which are low-pass-filtered at 0.15 Hz. (b) Seismograms which are bandpass-filtered between 0.2 and 1 Hz.

lations is that a shallow layer with parameters deduced from the inversion of the group velocity dispersion causes a regional amplification at long periods which is in agreement with the observed amplification. The signal duration is increased because of the dispersion of surface waves inside this layer.

DISCUSSION AND CONCLUSIONS

The analysis of seismograms shows the existence of a region in the southern part of the MVB where seismic signals are amplified. The southern limit of this region is situated near Tepoztlán and corresponds to the geographical limit of the MVB. The northern limit of the region is located near Teotihuacán. This delimitation is also supported by a strong

difference in the signal duration for earthquakes located in the Valley of Mexico and recorded north and south of the valley. Group and phase velocities in the period range 2–13 s are smaller in the southern part of the MVB than in the northern part. Although we could not measure directly the velocity in the region south of the MVB, the values of the phase velocity for the path Iguala–UNAM and the group velocity measured for the region between the Guerrero coast and Mexico City by Campillo *et al.* (1996) suggest that the velocities south of Tepoztlán are close to those measured in the northern part of the MVB. The low-velocity zone can be associated with the region of active volcanism in the southern part of the MVB. The northern limit of this zone corresponds, approximately, to the limit between the two different parts of the MVB deduced from geological data (Robin 1981). The

(a) low-pass at 0.15 Hz

(b) band-pass 0.2-1 Hz

Vertical component

Vertical component

Model structure

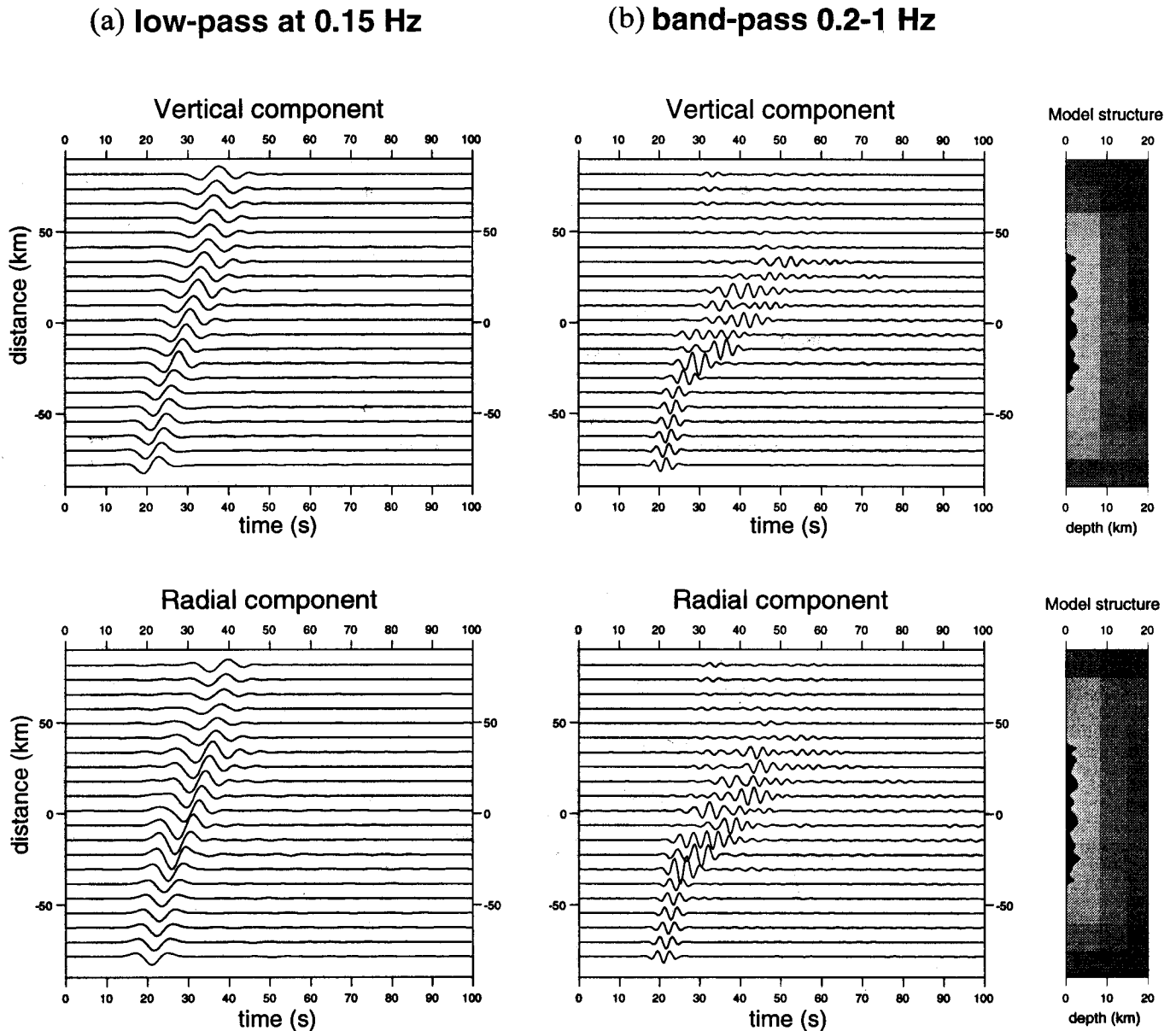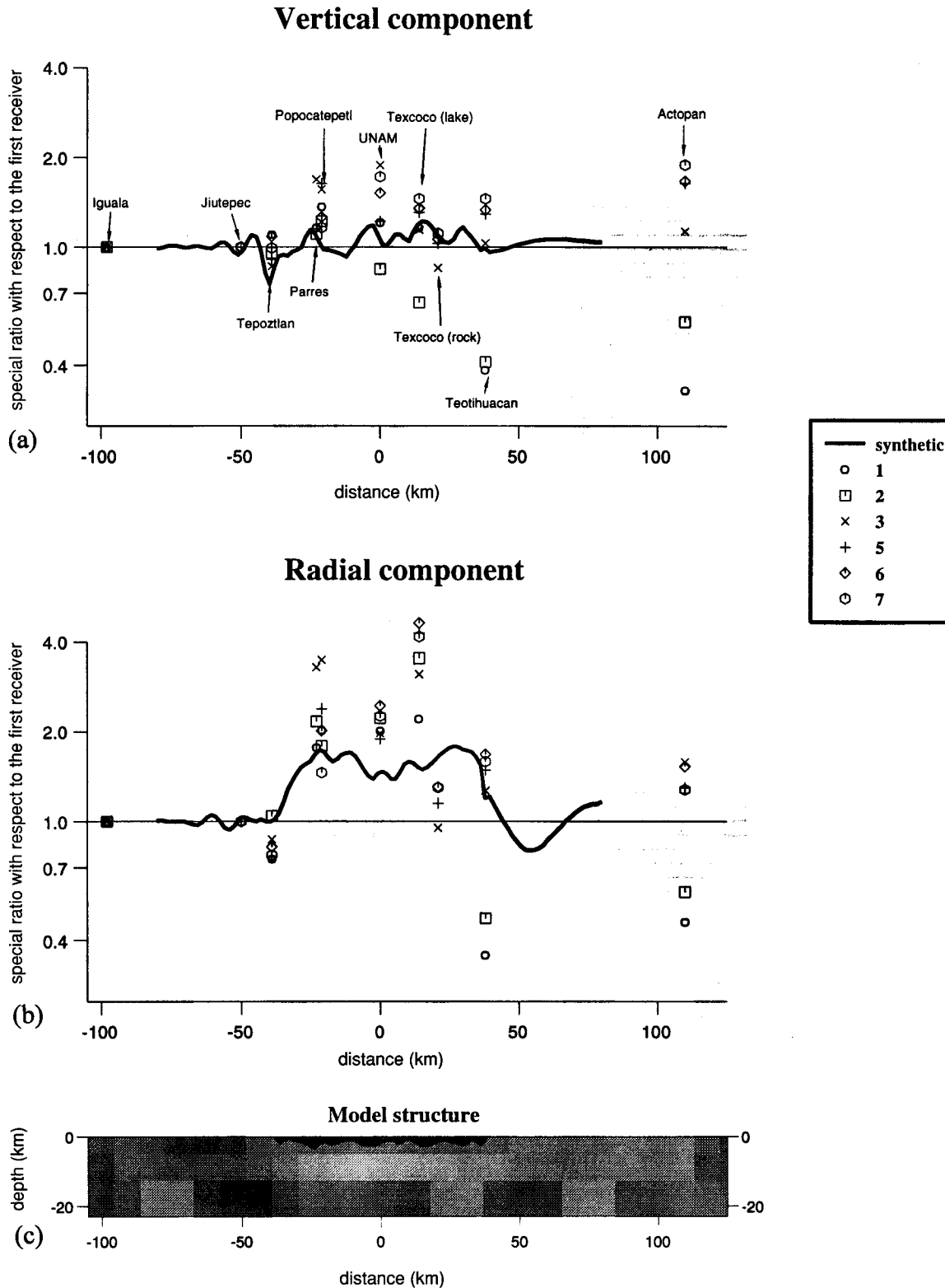### Radial component

Radial component

Model structure

Figure 12. As Fig. 11, but for a shallow low-velocity layer with an irregular basement.

inversion of the group velocity dispersion curves measured in the northern and southern parts of the MVB shows that the difference in velocities is due to the presence of a superficial low-velocity layer (with an average *S*-wave velocity of 1.7 km s^{-1} and an average thickness of 2 km) in the southern part of the MVB.

The numerical simulations show that this superficial low-velocity layer causes a regional amplification of the 8–10 s period signal which is of the same order as the amplification measured from the data. It also increases the signal duration because of the dispersion of surface waves. These results confirm the hypothesis of Singh *et al.* (1995), who suggested that the regional amplification observed in the vicinity of Mexico City is due to the anomalously low shear-wave velocity in the shallow volcanic rocks of the southern MVB.

Vertical component

(a)

Radial component

(b)

Model structure

(c)

Figure 13. Comparison of calculated and observed amplifications of seismic waves in the MVB at long periods (8–10 s). (a) Amplification for the vertical component. (b) Amplification for the radial component. (c) Model cross-section.

REFERENCES

Barker, J.S., Campillo, M., Sánchez-Sesma, F.J., Jongmans, D. & Singh, S.K., 1996. Analysis of wave propagation in the Valley of Mexico from a dense array of seismometers, *Bull. seism. Soc. Am.*, submitted.

Campillo, M., Singh, S.K., Shapiro, N., Pacheco, J. & Herrmann, R.B., 1996. Crustal structure south of the Mexican Volcanic Belt, based on group velocity dispersion, *Geofis. Intern.*, 35, 361–370.

Demant, A., 1981. L'Axe Néo-Volcanique Transmexicain. Etude volcanologique et pétrographique. Signification géodynamique, *Thèse de doctorat*, Université de droit, d'économie et des sciences d'Aix-Marseille, Marseille.

Dziewonski, A., Bloch, S. & Landisman, N., 1969. A technique for the analysis of transient seismic signals, *Bull. seism. Soc. Am.*, 59, 427–444.

Havskov, J. & Singh, S.K., 1978. Shallow crustal structure below Mexico City, *Geofis. Intern.*, 17, 223–229.

Herrmann, R.B., 1987. *Computer Programs in Seismology*, Saint Louis University, Missouri.

Jongmans, D., Demanet, D., Horrent, C., Campillo, M. & Sanchez-Sesma, F.J., 1996. Dynamic soil parameters determination by geophysical prospecting in Mexico City: implication for site effect modeling, *Soil Dynamics and Earthquake Engineering*, 15, 549–559.

Levshin, A.L., Yanovskaya, T.B., Lander, A.V., Bukchin, B.G., Barmin, M.P., Ratnikova, L.I. & Its, E.N., 1989. Recording, identification, and measurement of surface wave parameters, in *Seismic surface waves in a laterally inhomogeneous Earth*, pp. 131–182, ed. Keilis-Borok, V.I., Kluwer Academic Publisher, Dordrecht.

Lomax, A.J. & Snieder, R., 1994. Finding sets of acceptable solutions with a genetic algorithm with application to surface wave group dispersion in Europe, *Geophys. Res. Lett.*, 21, 2617–2620.

Lomax, A. & Snieder, R., 1995. The contrast in upper mantle shear-wave velocity between the East European Platform and tectonic Europe obtained with genetic algorithm inversion of Rayleigh-wave group dispersion, *Geophys. J. Int.*, 123, 169–182.

Ordaz, M. & Singh, S.K., 1992. Source spectra and spectral attenuation of seismic waves from Mexican earthquakes, and evidence of amplification in the hill zone of Mexico City, *Bull. seism. Soc. Am.*, 82, 24–43.

Pedersen, H.A., Campillo, M. & Sánchez-Sesma, F.J., 1995. Azimuth dependent wave amplification in alluvial valleys, *Soil Dynamics and Earthquake Engineering*, 14, 289–300.

Poupinet, G., Ellsworth, W.L. & Fréchet, J., 1984. Monitoring velocity variations in the crust using earthquake doublets: An application to the Calaveras fault, California, *J. geophys. Res.*, 89, 5719–5731.

Robin, C., 1981. Relations volcanologie–magmatologie–géodynamique: application au passage entre volcanismes alcalin et andésitique dans le sud mexicain, *Thèse de doctorat*, Université de Clermont-Ferrand II, Clermont-Ferrand.

Singh, S.K. & Ordaz, M., 1993. On the origin of long coda observed in the lake-bed strong motion records of Mexico city, *Bull. seism. Soc. Am.* 83, 1298–1306.

Singh, S.K., Quass, R., Ordaz, M., Mooser, F., Almora, D., Torres, M. & Vasquez, R., 1995. Is there truly a 'hard' rock in the Valley of Mexico, *Geophys. Res. Lett.*, 22, 481–484.

Stange, S. & Friederich, W., 1992. Guided wave propagation across sharp lateral heterogeneities: the complete wavefield at a cylindrical inclusion, *Geophys. J. Int.*, 111, 470–482.

Tardy, M., 1980. Contribution à l'étude géologique de la Sierra Madre Orientale du Mexique, *Thèse d'Etat*, Université Pierre et Marie Curie, Paris.

APPENDIX A: LOGARITHMIC STACKING OF PERIOD–GROUP VELOCITY DIAGRAMS

To enhance the period–time diagrams, we use a logarithmic stacking in the period–time domain technique (Campillo *et al.*

1996) based on the frequency–time analysis described by Levshin *et al.* (1989). In frequency–time analysis (Levshin *et al.* 1989), the spectrum of the signal is multiplied by a narrow Gaussian window centred at period T, and then the inverse Fourier transform is computed. These two steps are repeated for a large number of periods T, thus obtaining a function of time and period, $A(t, T)$. The amplitude of this function is used for the graphic representation of the signal in the period–time domain.

We calculate a mean period–time envelope, $As(t, T)$, as the product of the normalized envelopes of the n records used:

$$As(t, T) = N_1(t, T) \times N_2(t, T) \times \ldots \times N_n(t, T), \tag{A1}$$

where $N_i(t, T)$ is the normalized envelope of record i. This procedure is called logarithmic stacking.

Let us assume that, at a given period T, the envelopes have the theoretical Gaussian shape with the same width parameter a and the maxima at times τ_i (group time at period T):

$$N_i(t, T) = \exp[-(t - \tau_i)^2/2a^2]. \tag{A2}$$

Combining eqs (A1) and (A2), we can see that, if the group time τ_i is the same for all the records, the resulting envelope has a unit maximum value and a bandwidth equal to $a/\sqrt{n}$. If the group times τ_i differ, the maximum amplitude of the resulting envelope is smaller than 1. Let us consider the group times τ_i distributed around a mean value τ_0:

$$\tau_i = \tau_0 + \delta_i, \tag{A3}$$

where δ_i is the deviation of the group time for each record. In this case, the mean envelope has the maximum at the time τ_0 with an amplitude equal to

$$\text{Max}(A_s(t, T)) = \exp\left[\frac{-\sum\limits_{i=1}^{n} \delta_i^2}{2a^2}\right]. \tag{A4}$$

The resulting period–time envelope has strong amplitudes in the narrow region where coherent arrivals exist and small amplitudes for periods where the coherence between different signals disappears. Therefore, this method allows a better definition of the period–time range for which a stable arrival is observed on all the records. An additional advantage of this technique is that the amplitude of the mean envelope at a given period depends on the variance of group times (eq. A4). Therefore, this variance can be measured directly from the amplitude of the stacked period–time diagram. The logarithmic stacking allows a direct evaluation of uncertainty of the group time.

Using one period–group velocity diagram, we estimate a dispersion of the group time. At each period T, the value of the group time $\tau(T)$ is estimated as the time where the amplitude of $A(t, T)$ (in the case of a one-record diagram) or $As(t, T)$ (in the case of a stacked one) has its maximum.

The uncertainty of the group time is a main source of error during the group velocity measurement. To estimate this uncertainty from a one-record period–time diagram, we define the interval of possible values of group time at each period T as the interval where the amplitude of the function $A(t, T)$ is larger than 95 per cent of its maximum. An estimation of the uncertainty on the group time can also be made in the case of a stacked diagram using eq. (A4).

APPENDIX B: Group velocity measurement

We apply frequency–time analysis to measure dispersion curves of the group time $\tau(T)$ and its uncertainty. We can use one- or two-station measurement to obtain the value of the group velocity. In the first case, we apply the formula

$$\tau(T) = d/U(T), \tag{B1}$$

where d is the epicentral distance and $U(T)$ is the group velocity at period T. In the second case, we measure group times τ_1 and τ_2 at each of the two selected stations. The interstation group velocity is then the ratio of the interstation distance to the difference between those group times:

$$U(T) = \frac{(d_2 - d_1)}{[\tau_2(T) - \tau_1(T)]}, \tag{B2}$$

where T is the period and d_1 and d_2 are the epicentral distances for each station.

APPENDIX C: PHASE VELOCITY MEASUREMENT

To measure interstation phase velocities, we apply the cross-spectrum method. The phase of the cross-spectrum gives the frequency-dependent time delay between two stations:

$$\delta t(\omega) = \frac{\varphi(\omega)}{i\omega}. \tag{C1}$$

The phase velocity $C(\omega)$ is therefore given by

$$C(\omega) = \frac{(d_2 - d_1)}{\delta t(\omega)}, \tag{C2}$$

where ω is the angular frequency, $\delta t(\omega)$ is the time delay, $\varphi(\omega)$ is the phase of the cross-spectrum, and d_1 and d_2 are the epicentral distances for each station. The coherence between the two signals is calculated to control the quality of the measurement. The measurements are performed only in the period range where the value of the coherence is close to 1.

An important improvement in the quality of such measurements can be obtained by a preliminary filtering of the signals. Following Levshin *et al.* (1989), we filter the data in the frequency–time domain to isolate the fundamental mode of the Rayleigh wave.

Finally, group velocity is related to phase velocities by

$$U(\omega) = C(\omega)/\left[1 - \omega\frac{\partial C(\omega)}{\partial\omega}/C(\omega)\right]. \tag{C3}$$

In this case, an average velocity between two stations and an estimation of the error are obtained as an average value and a standard deviation of individual dispersion curves measured from records of different events on different components. The averaging is done using the values of coherence as weights.